


Article

Investigation on the Properties of Flame-Retardant Phase Change Material and Its Application in Battery Thermal Management

Yilin Cui ^{1,2}, Yin Chen ^{1,2,*}, Luyao Zhao ^{1,2}, Fang Zhu ^{1,2}, Lixia Li ^{1,2}, Qinghong Kong ^{1,2} and Mingyi Chen ^{1,2,*} ¹ School of Emergency Management, Jiangsu University, Zhenjiang 212013, China² School of the Environment and Safety Engineering, Jiangsu University, Zhenjiang 212013, China

* Correspondence: 1000005956@ujs.edu.cn (Y.C.); chenmy@ujs.edu.cn (M.C.)

Abstract: The thermal safety problem of lithium-ion batteries (LIB) in use requires an excellent thermal management system to preserve it. In the paper, an expansion flame-retardant composed of APP and CFA and kaolinite is used to enhance the flame-retardant property of phase change materials (PCM). The performances of PCM and their property in the thermal management of LIB were studied. The results indicate that the kaolinite can improve the long-term thermostability of PCM. The addition of flame retardant can make the flame-retardant property of PCM reach V0 level. The synergistic action of expansion flame-retardant and kaolinite can increase the residual carbon and enhance the thermal reliability of flame-retardant PCM (RPCM). The RPCM has an obvious cooling effect on the surface temperature of the battery. The RPCM can reduce the maximum temperature of the cell to 37.4 °C at 3 C, which is 12 °C lower than pure PA. The peak temperature of the battery pack at 3 C is also reduced to 50.28 °C by the flame-retardant PCM, and the temperature difference is kept within 5 °C.

Keywords: flame-retardant; phase change materials; thermal management; kaolinite; lithium-ion battery pack



Citation: Cui, Y.; Chen, Y.; Zhao, L.; Zhu, F.; Li, L.; Kong, Q.; Chen, M. Investigation on the Properties of Flame-Retardant Phase Change Material and Its Application in Battery Thermal Management. *Energies* **2023**, *16*, 521. <https://doi.org/10.3390/en16010521>

Academic Editor: Manolis Souliotis

Received: 1 December 2022

Revised: 27 December 2022

Accepted: 28 December 2022

Published: 3 January 2023



Copyright: © 2023 by the authors. Licensee MDPI, Basel, Switzerland. This article is an open access article distributed under the terms and conditions of the Creative Commons Attribution (CC BY) license (<https://creativecommons.org/licenses/by/4.0/>).

1. Introduction

The emergence of eco-crises such as global warming and energy crises such as excessive dependence on fossil fuels has promoted great attention and the development of new energy since the 21st century [1,2]. Lithium-ion batteries (LIB) have been extensively studied for their advantages of high specific energy density, low self-discharge rate and long cycle life. Nevertheless, battery performance, life cycle and reliability are closely related to temperature during use [3,4]. Abnormal temperature may cause capacity power attenuation, battery pack temperature difference, and thermal runaway. In particular, the heat does not timely dissipate during the LIB operation, which will bring serious harm resulting in thermal runaway or explosion [5,6]. Therefore, heat accumulation is reduced by adding a battery thermal management system (BTMS), making it better for practical use [7,8].

BTMS is divided into three main categories according to the difference of heat transfer medium: air, liquid and phase change material (PCM) BTMS [9,10]. There also have other cooling methods originating from the three categories, such as heat pipe cooling and micro-channel cooling [11]. Bibin et al. [12] innovatively analyzed a double-potential battery by using computational fluid dynamic (CFD) software, added an air blast cooling system to the batteries, and observed the changes in its surface temperature. They found that forced air cooling could effectually reduce the temperature of the batteries. Ding et al. [13] studied the effect of liquid-cooled channel structure on battery pack temperature to improve the management effect of liquid cooling and heat. They found that a rectangular channel more easily decreases the peak temperature of battery pack, and the reduction degree is positively correlated with the length–width of rectangular channel. However, air cooling and liquid cooling as

active cooling systems require additional devices such as fans, pipes, pumps, and valves, which further increase weight and space requirements. PCM cooling has merits including lower energy, larger storage capacity, no additional device, and effectively controlling the maximum temperature compared with other cooling methods. Researchers have carried out more studies on this [14,15]. Ianniciello et al. [16] compared PCM with other thermal management systems to study the thermal management effect of PCM. The results show that PCM can well reduce the peak temperature of LIB surface and the temperature difference between batteries. However, PCM has the disadvantages of low thermal conductivity and easy leakage. So, researchers can improve the performance of PCM by preparing composite PCM or combining with other thermal management methods. Chen et al. [17] use graphene and graphite nanosheets to collaboratively boost the heat-conducting property of the PCM to obtain high thermal conductivity PCM. The result showed that the peak temperature of the cell module and the temperature difference of the batteries could be effectively reduced by using composite phase change material (CPCM). Zou et al. [18] synthesized a new type of high thermal conductivity composite PCM and studied its local heat transfer characteristics to the battery pack to ensure the low leakage rate and high thermal conductivity of phase change materials. The results indicated that the increase in PCM can reduce the temperature difference by 46.7%. Li et al. [19] prepared the shaped composite by using stearic acid and kaolinite to study the effect of particle size distribution on PCM performance. The results showed that kaolinite with a uniform grain size is helpful to establish the thermal conduction path and improve the heat stability of the material. Furthermore, some studies have ameliorated PCM shortcomings by coupling with other cooling techniques. Weng et al. [20] improved the performance of PCM by coupling liquid cooling, and the results indicated that it still has a fine effect at high temperatures. Mei et al. [21] used PCMs in combination with fins to verify the effect of the different BTMS and found that the coupling fin can reduce the battery surface temperature by 35.5%. Qu et al. [22] devised a fresh heat pipe of the three-dimensional oscillation and coupled it with PCMs to study the effect on the properties of PCMs. The results indicated that the addition of oscillating heat pipe could increase the melting time of paraffin wax and reduce the curing time. PCM has the disadvantages of low thermal conductivity, easy leakage, and flammability. At present, PCM has a good effect on improving thermal conductivity, and can achieve good results in battery thermal management. However, the flammability of the PCM will promote thermal runaway propagation in the case of thermal runaway. This will create a greater risk, so we hope to solve this contradiction by making flame-retardant materials.

A common way is currently to mix flame-retardant additives to PCM to inhibit their flammability [23]. Halogen-free flame retardants have been widely used in view of the harm of organic halogen flame-retardants to environmental safety. Among them, phosphorus and nitrogen flame retardants have been researched because of their advantages of environmental protection, low price, and small additive amount. Ammonium polyphosphate (APP) is an inorganic macromolecule flame-retardant containing a lot of phosphorus and nitrogen. It acts as an acid source and air source in the expandable flame-retardant system, and can be used together with other carbon sources to achieve a flame-retardant effect. APP is flame-retarded by condensed phase and gas phase. On the one hand, non-volatile phosphorus and polyphosphoric acid are used to cover the material surface during thermal expansion to isolate the air. On the other hand, nitrogen and ammonia are decomposed to dilute the oxygen in the air to achieve a flame-retardant effect [24,25]. Jia et al. [26] used lignin fiber, APP, diphenyl phosphate, and silica aerogel on flame-retardant low-density polylactic acid (PLA) to enhance the PLA flame-retardant performance. The results indicated that the addition of APP can boost the flame-retardant performance of PLA at a lower flame-retardant dosage. Fan et al. [27] compounded a fresh type of carbon-forming agent to promote the IFR carbon formation efficiency, which is combined with APP, polypropylene, and melamine pyrophosphate to flame-retardant polypropylene. The results showed that the composite has a good flame-retardant effect. Kaolinite is a fine clay mineral with two layers of crystals: a silica oxide tetrahedral layer and an alumina octahedral layer. Kaolinite can be used in expansion

flame-retardant system to enhance the flame-retardant effect [27–30]. Zia-ul-Mustafa et al. [31] researched the influence of kaolinite and clay on the expansion flame-retardant coating to boost the flame-retardant layer formulation. The results indicated that the kaolinite and clay can help to enhance the fire resistance of the layer.

At present, aerogels, thermal insulation wool, and other materials have been used in battery modules to isolate heat and reduce the spread of thermal runaway between batteries [32,33]. However, in practical applications, not only the harm of extreme conditions should be considered, but also the electrochemical performance and life of the battery in operation are important factors. The temperature difference caused by heat insulation will affect the normal use of the battery. Therefore, flame-retardant composite PCMs can be used in battery modules to reduce heat transfer.

A new flame-retardant composite phase change material (PA/EG/IFR/Kaolinite) (RPCM) has been prepared in this paper. EG is used as a high thermal conductivity additive and support material, and the expansion flame retardant composed of APP and CFA is used as a flame-retardant material together with kaolinite. The result of different amounts of flame retardants and kaolin on thermal stability, flame retardancy, and latent heat of phase change materials were studied. Its influence on surface temperature and temperature difference of battery pack in thermal management of lithium-ion battery was studied. The effect of the introduction of kaolin on the comprehensive properties of phase change materials and its practical application were observed.

2. Experiment

2.1. Materials and Preparation of RPCMs

PA, which has a melting point of 46 °C and the latent heat of 210 J·g^{−1}, was purchased from Hebei Haoyu New Energy Technology Co., Ltd. (Hebei, China). Expanded graphite (EG) was provided by Qingdao Tengshengda Carbon Machinery Co., Ltd. (Shandong, China), with a purity of 99%. APP was purchased from Shanghai Linen Technology Development Co., Ltd. (Shanghai, China), and kaolinite from Shandong West Asia Chemical Industry Co., Ltd. (Shandong, China). The carbon forming agent (CFA) was self-made in the laboratory, and the preparation process is shown in the following paragraph. Cyanuric chloride and ethanol amine were purchased from Shanghai Aladdin Biochemical Technology Co., Ltd. (Jiangsu, China). Acetone and sodium hydroxide were purchased from Sinopharm Chemical Reagent Co., Ltd. (Jiangsu, China). Hexamethylene-diamine was purchased from Shanghai Macklin Biochemical Co., Ltd. (Shanghai, China).

Preparation process of carbon-forming agent:

An amount of 0.1 mol cyanuric chloride and 50 mL acetone was added to a three-neck flask. Amounts of 0.1 mol of ethanol amine and 0.1 mol of sodium hydroxide were mixed in water and added to the flask by drops, and reacted at 0–5 °C for two hours. After that, 0.05 mol hexamethylene-diamine and 0.1 mol sodium hydroxide were mixed in water, added to the flask, and reacted at 40–50 °C for 10 h. Finally, 0.05 mol hexamethylene-diamine and 0.1 mol sodium hydroxide aqueous solution were added into the flask for reflux for 10 h. The compound was filtered and washed with water to obtain CFA after cooling down to room temperature [34].

The RPCM uses PA as the main energy storage material and EG as the adsorption material of paraffin wax to prevent its leakage at high temperature. Meanwhile, the expansion flame-retardant (abbreviation is IFR) was selected as the flame-retardant for the preparation of RPCM. The composition of IFR included APP and CFA, and the ratio was 4:1. Kaolinite was added to improve thermal stability and flame retardancy. Figure 1 shows the preparation process of RPCM, and Table 1 shows the material proportion and naming method of RPCM.

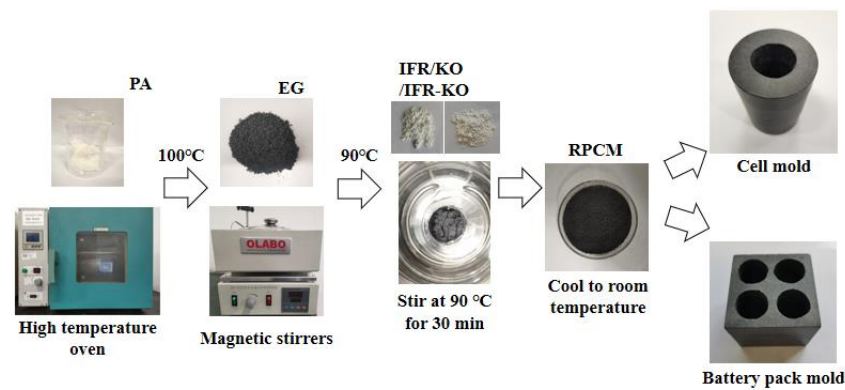


Figure 1. RPCMs preparation process.

Table 1. Composition of RPCM.

Materials	No.	Paraffin (%)	EG (%)	Kaolinite (%)	IFR (%)
KPCM	K1	93	7	0	\
	K2	92	7	1	
	K3	91	7	2	
	K4	90	7	3	
RPCM	R1	83	7	0	10
	R2	73	7	0	20
	R3	63	7	0	30
	R4	80	7	3	7
	R5	70	7	3	17
	R6	60	7	3	27

A definite proportion of PA was weighed and was added to a beaker. We let it melt at 100 °C for 30 min. Then, the beaker was moved to a 90 °C magnetic stirrer and the expanded graphite was added in twice to make sure the material was evenly mixed. IFR or kaolinite mixture was then added and stirred. After cooling to room temperature, RPCM was obtained. The material was pressed into different shapes as needed.

2.2. Performance Testing and Characterization

If the CPCM used in BTMS has serious leakage, it will not only reduce the heat dissipation effect of the LIB, but also cause the LIB short circuit, affecting the battery safety. The macroscopic thermal stability of kaolinite composite PCM with different mixing ratios was investigated and tested. The prepared composite PCM was placed on filter paper and put into a drying oven at 80 °C for long-term leakage test. The sample quality was weighed every 10 h. The weighing precision of electronic balance was 0.1 mg.

X-ray Diffraction (XRD) is a technical means to analyze the composition and internal crystal structure of a material. X-ray diffraction is used to diffract a material to obtain its diffraction pattern in the material to analyze the material. The Bruker D8 ADVANCE X-ray diffractometer was used to test the composite PCMs. The diffraction Angle $2\theta = 10\sim 60^\circ$ and the scanning rate was $5^\circ\text{C}\cdot\text{min}^{-1}$.

UL vertical combustion test is an important index to measure the flame retardancy of materials. This sample was prepared according to GB/T2408-2008 standard specification and performed UL-94 vertical combustion test using CZF-1 vertical combustion tester. The sample was vertically clamped and exposed to the ignition source twice for 10 s each time. The results are classified as V-0, V-1, V-2, or NR (non-rated) combustion, with V-0 being the best combustion rating. JF-3 oxygen index instrument was used to test the limit oxygen index of the sample strip. A minimum concentration of oxygen was obtained in the form of LOI, which was only sufficient to support the combustion of the strip. The higher the LOI, the better the flame retardancy.

A multi-functional thermal conductivity tester (Xiangtan Dra-III model) was adopted for testing with an accuracy of less than or equal to 3%. The material was pressed formation two test samples with the diameter of 40 mm and the thickness of 8 mm. During the test, the sensor was placed between two identical samples and held down with a weight to prevent sensor movement from affecting the data. The average value was the thermal conductivity of the material after many measurements.

A synchronous thermal analyzer (STA 449F3) was used to test the potential heat and the phase change temperature. The test temperature range was from room temperature to 120 °C in nitrogen atmosphere, the heating rate is 10 °C·min⁻¹, and the temperature accuracy is ±0.1 °C and the enthalpy value is ±1%. A synchronous thermal analyzer (STA 449F3) was used to test the thermogravimetric of the sample. The weight of the sample was 3–5 mg, the heating rate was 10 °C·min⁻¹, the temperature range was 30–800 °C, nitrogen protection, the temperature accuracy was ±0.1 °C, and the balance accuracy was ±1%.

2.3. Construction and Testing of the Thermal Management Platform

Figure 2 shows an experimental diagram of the thermal management performance test of LIB. The test system includes battery charging and discharging equipment (CT4008, NEWARE TECHNOLOGY LIMITED, Shenzhen, China), biochemical incubator (SPX-50B, 0–60 °C, Tianjin Honuo), data acquisition module (7018, Hefei Flow layer) and 18,650 ternary lithium-ion battery used in the experiment. The battery used in this paper was an 18,650 lithium-ion battery purchased from Sanyo Company, and its nominal battery capacity was 2.0 Ah. Before the new battery was used, a charge–discharge cycle was carried out on the battery, and the battery was left for 24 h to ensure its stability. The battery thermal management module was carried out in an incubator with a set temperature of 25 °C (±0.5 °C). The cycle working step of battery charge–discharge cycle meter was: first constant discharge of electricity, until the voltage drops to 2.75 V, and then constant current constant voltage charge, stop charging when the current was less than 0.05 Ah. Discharge current was set as 1 C, 2 C, and 3 C according to the actual demand (C multiplier is the quantitative expression of charge–discharge current and its nominal capacity). The distribution of the thermocouple was shown in Figure 2, Each thermocouple was fixed in the middle position of the cell. Multiple thermocouples were set to evaluate the temperature difference inside the battery pack. Thermocouples were divided into one group (positions 1, 3, 5, 7) and two groups (positions 2, 4, 6, 8) according to their positions in the battery string. After the temperature difference of two group were calculated, the larger difference was the battery pack temperature difference.

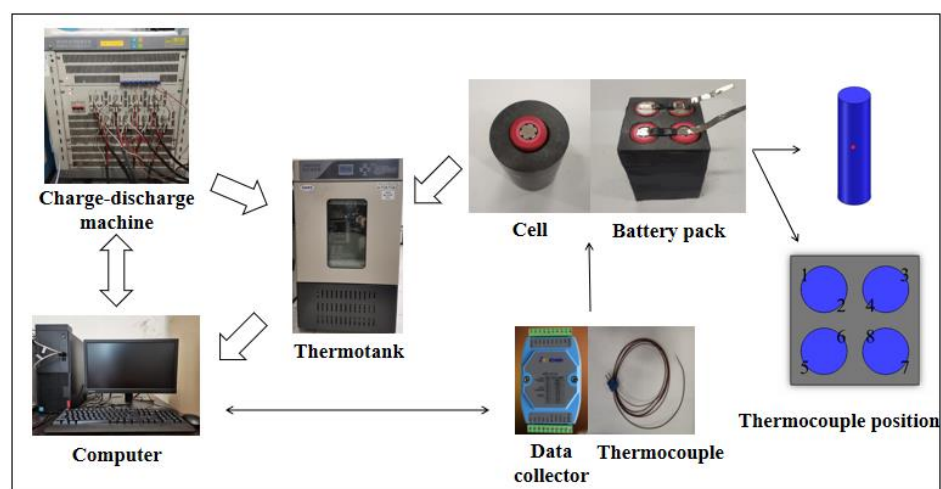


Figure 2. Thermal management system platform.

3. Results

3.1. Leakage Rate

Figure 3 shows the leakage rate curves of PCM with different proportions of kaolinite. After 10 h, there is leakage of PCMs. the leakage rate of PCM K1 without kaolinite is 1.5%, and the leakage rate of K2–K4 with different kaolinite proportions is 1.43%, 1.17%, and 1.08%, respectively. At the initial stage, the leakage rate of the four PCM is not very different, because the PCM uses EG as the adsorption material. The porous surface of EG can be used as PA carrier at high temperature to enhance the heat stability of PCM. Later, kaolinite showed its influence on the thermal stability of PCM during the long-term thermal cycle. After 110 h, the K1 leakage rate is 6.88%, while the K4 leakage rate is only 3.1%. The results indicate that kaolinite can improve the heat stability of PCM in the long period thermal cycle. This is because kaolinite can act as a barrier to prevent organic matter from leaking, thus improving material stability.

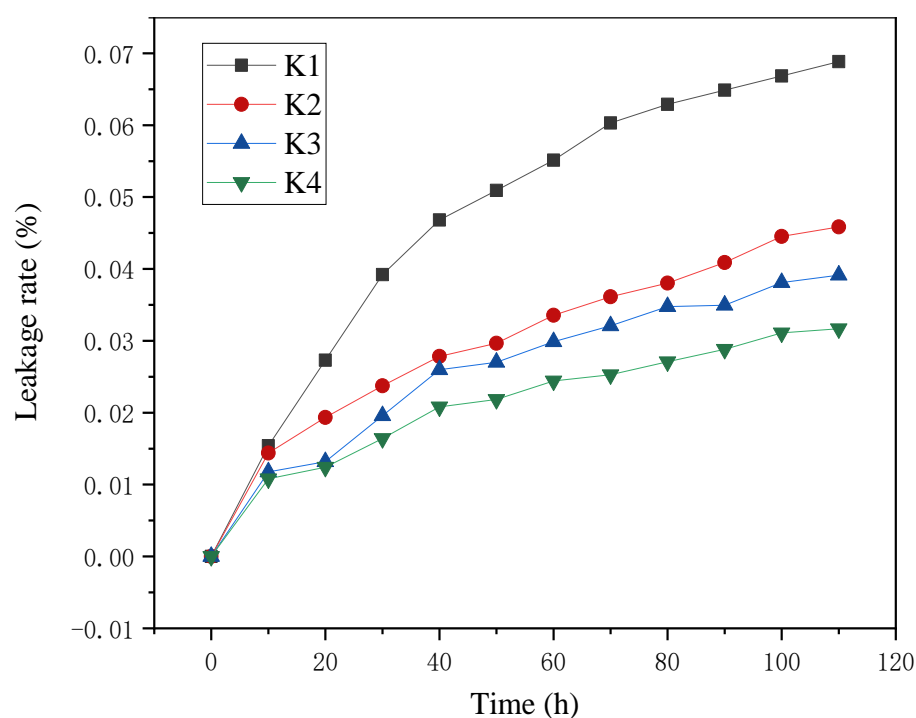


Figure 3. The leakage rate curve diagram.

3.2. XRD

The XRD results of RPCMs are shown in Figure 4. PA has a diffraction peak at 10.75° , 12.92° , 17.28° , 21.42° , and 23.69° , respectively, while EG only has an obvious diffraction peak at 26.49° . Flame-retardants peak at 14.65° and 15.48° . The flame-retardant PCM R1 showed the same diffraction peak at the same 2-Theta value as PA, EG and IFR, and no new peak appeared. It is also observed that the diffraction peaks of R2 and R3 at 14.65° and 15.48° are enhanced with the increase in the proportion of flame-retardants. Kaolinite has no obvious peak value. Therefore, R4, R5 and R6 also show diffraction peaks at the same 2-Theta value as R1, and there are no new diffraction peaks. The diffraction peaks of PCM at 14.65° and 15.48° are also different due to the difference in the amount of flame-retardants added. No new diffraction peak is generated in all PCM, manifesting that no chemical reaction occurred in the synthesis process of PCM and no new substance is formed.

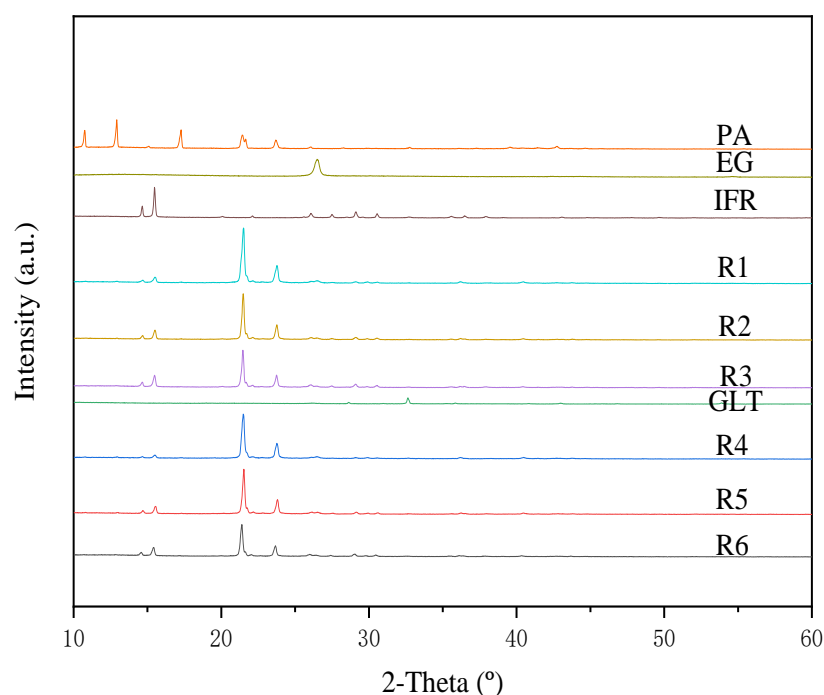


Figure 4. XRD graph.

3.3. The LOI and the UL-94

Table 2 exhibits the LOI and UL-94 test results of flame-retardant PCMs. The LOI value of pure paraffin wax is 18.2% and there is no UL-94 grade. The LOI value of the RPCM is proportional to the amount of flame-retardant. When the amount of flame retardant reaches 30%, the LOI value of R3 reaches 29.8%, which is the level of V0. R1 and R2 have LOI values of 25.3% and 27.6%, respectively, and vertical combustion levels of V2 and V0, respectively. After the addition of kaolinite, the LOI value of RPCM is increased, and the LOI values of R4 and R5 are 25.5% and 28.1%, and the vertical combustion grades are V2 and V0. R6 has a LOI value of 31.3% and a vertical combustion rating of V0. This is mainly due to the expansion flame-retardant system forms a porous expanded carbon layer on the material surface. Carbon layer can inhibit the release of flammable gas and the diffusion of oxygen to the material surface and slow the thermal decomposition rate of the material. Kaolinite is distributed on the surface, forming a barrier that prevents the release of combustible gases and the escape of organic matter, further enhancing the carbon layer. Thus, it can cooperate with expansion flame-retardants to act as material flame-retardants. Li et al. [35] added 20% expansion flame retardant to make the vertical combustion level of the material reach V0. In this paper, the material can reach V0 level when the addition level reaches 20%.

Table 2. LOI and UL-94 results.

	PA	R1	R2	R3	R4	R5	R6
LOI	18.2%	25.3%	27.6%	29.8%	25.5%	28.1%	31.1%
UL-94	NR	V2	V0	V0	V2	V0	V0

3.4. Thermal Conductivity and DSC

The thermal conductivity test results of RPCM are shown in Figure 5. The thermal conductivity of PA is $0.266 \text{ W} \cdot \text{m}^{-1} \cdot \text{K}^{-1}$. The heat-conducting property of RPCM increases obviously due to the participation of high thermal conductivity additive EG. However, the improvement of heat-conducting property of RPCM is mainly EG, and the content is the same, so the thermal conductivity of flame-retardant PCM is little different, distributed between $1.27 \text{ W} \cdot \text{m}^{-1} \cdot \text{K}^{-1}$ and $1.3 \text{ W} \cdot \text{m}^{-1} \cdot \text{K}^{-1}$. The thermal conductivity of R1–R6 is 1.272, 1.272, 1.283, 1.306, 1.278, and $1.284 \text{ W} \cdot \text{m}^{-1} \cdot \text{K}^{-1}$, respectively. Compared with PA, the

thermal conductivity is improved by 378–390%. It is found that the thermal conductivity increased slightly after kaolinite is added. This is because kaolinite fills the gaps between the large crystals and is used to connect the different crystals. This will facilitate the construction of continuous heat conduction channels in the material and increase the heat transfer rate. Weng et al. [20] obtained the thermal conductivity of $1.26 \text{ W}\cdot\text{m}^{-1}\cdot\text{K}^{-1}$ by adding 6% EG when preparing composite phase change materials. Thermal conductivity is between $1.27\text{--}1.30 \text{ W}\cdot\text{m}^{-1}\cdot\text{K}^{-1}$ when 7% EG is added, which shows some improvement.

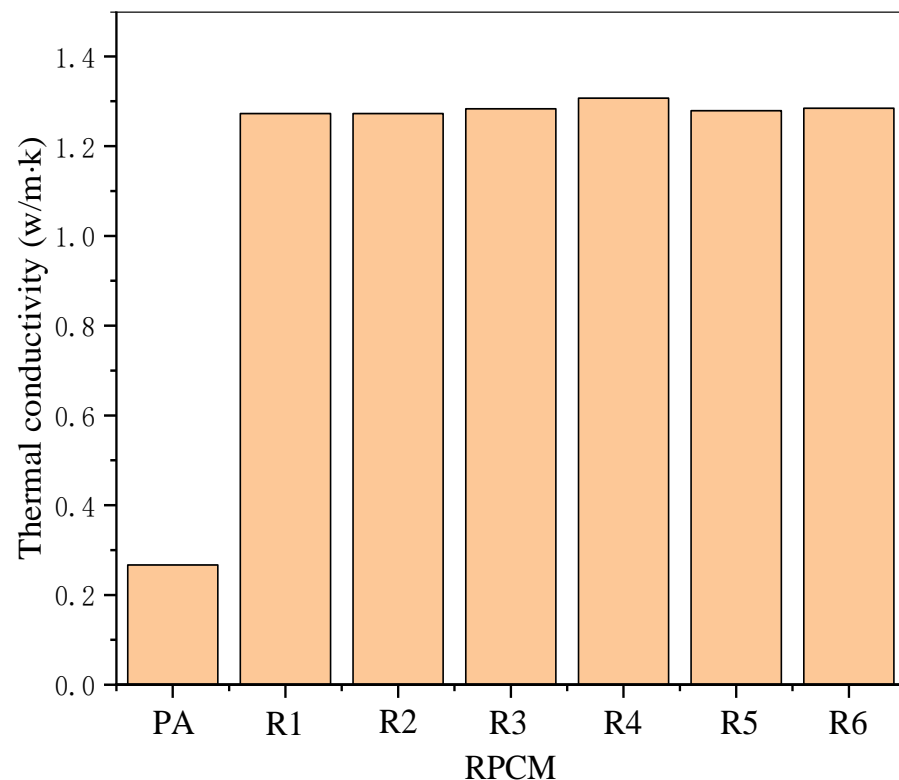


Figure 5. Thermal conductivity of RPCM.

Figure 6 shows the DSC curve of flame-retardant PCM. It can be observed that the potential heat of flame-retardant PCM is lower than that of PA, and the melting point is lower. The latent heat of flame-retardant PCM R1–R6 is $170.3 \text{ J}\cdot\text{g}^{-1}$, $155 \text{ J}\cdot\text{g}^{-1}$, $130.1 \text{ J}\cdot\text{g}^{-1}$, $169.4 \text{ J}\cdot\text{g}^{-1}$, $147.3 \text{ J}\cdot\text{g}^{-1}$, and $121 \text{ J}\cdot\text{g}^{-1}$, respectively. The decrease in latent heat of flame-retardant PCM is mainly because the latent heat value is mainly related to the proportion of paraffin wax. As the main source of potential heat of flame-retardant PCM, the decrease in the content of paraffin wax also reduces the latent heat value. Therefore, the latent heat value of flame-retardant PCM can be obtained theoretically by calculating the paraffin content, and the difference between the measured results and the theoretical calculated values is very small in this paper. The melting point of all flame-retardant PCM moves like low temperature, which is related to the improvement of thermal conductivity. The addition of high thermal conductive material makes the heat transfer inside the material faster, so the melting point of flame-retardant PCM is shift.

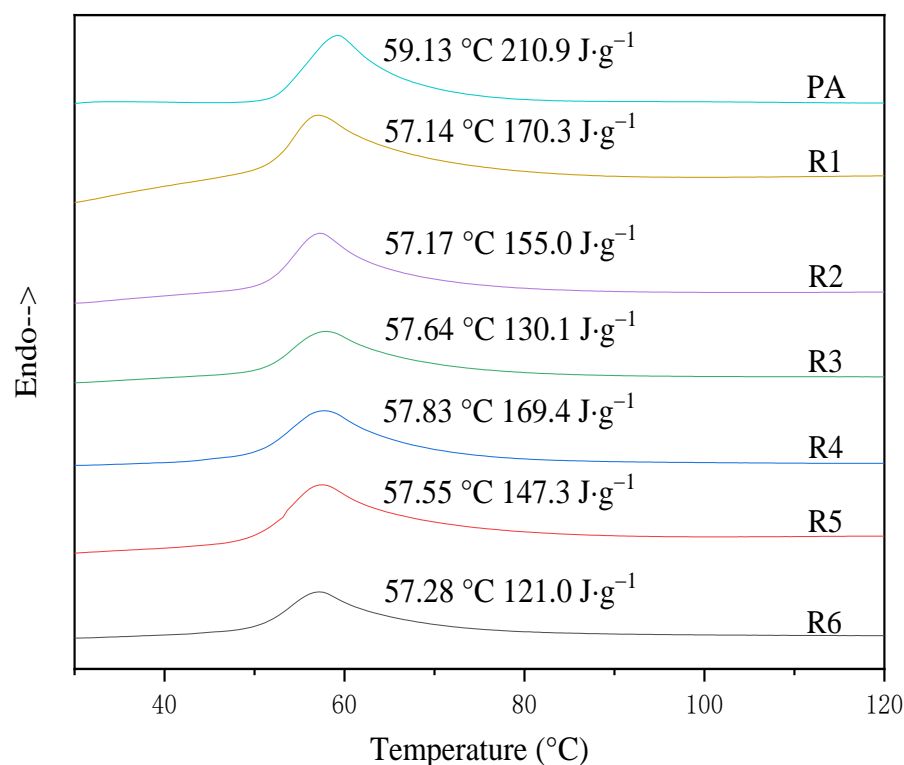


Figure 6. DSC curve.

3.5. TG

The TG curve of flame-retardant PCM is shown in Figure 7, and other details are listed in Table 3. Observing Figure 7, the PCM degrades between 200 °C and 400 °C, because the gasification and pyrolysis of paraffin. Pure paraffin leaves only 2.3% carbon after decomposition. The addition of flame-retardant boosts the heat stability of the material, and the residual carbon content of R1, R2 and R3 increases. The addition of kaolinite also enhanced the heat stability of RPCM. It can be observed from Table 3 that the specific temperature of different weight loss during the decomposition of PCM. It is found that the flame-retardant PCM $T_{-5\%}$, $T_{-25\%}$, and T_p are all larger than that of pure paraffin, indicating that the addition of flame-retardants and kaolinite improves the thermal stability of paraffin. In addition, R6 has a maximum carbon residue of 22.3% at 800 °C, which means it has superior carbon formation capacity. It is mainly because the synergistic flame retardancy of the expansion flame-retardant system and kaolinite. It can be inferred that in the process of temperature rise, APP decomposition releases ammonia and water, and generates phosphoric acid, which is esterified and cross-linked with CFA to form carbon layer and protect the matrix. Kaolinite acts as a barrier on the surface to prevent organic matter from escaping. The synergistic action of the expansion flame-retardant system and kaolinite can form a denser barrier to reduce the combustion rate, reduce the heat release, and improve the thermal reliability of PCMs.

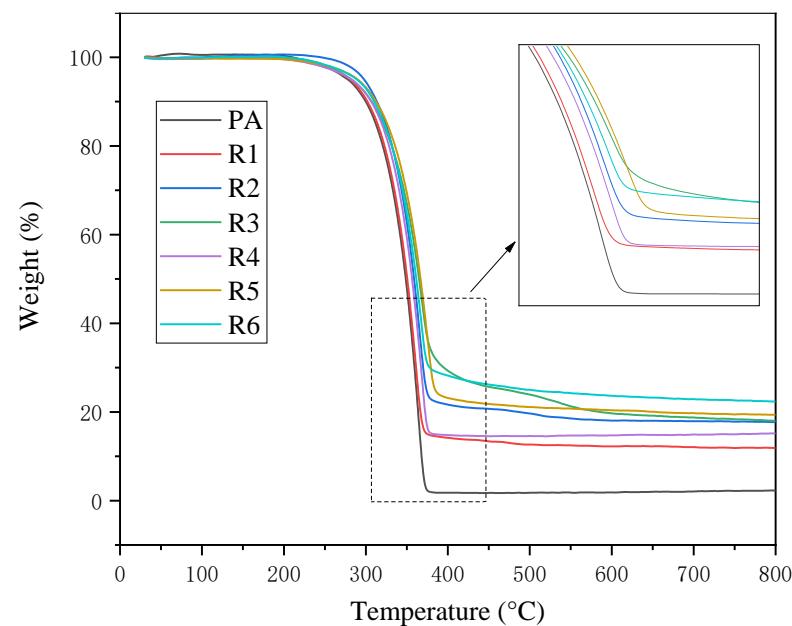


Figure 7. TG curve.

Table 3. Specific thermogravimetric parameters of PCMs.

Sample	T _{-5%} (°C)	T _{-50%} (°C)	T _p (°C)	Char Residue at 800 °C
PA	277	348	375	2.3%
R1	280	350	380	11.8%
R2	283	358	382	17.6%
R3	282	359	440	17.8%
R4	281	356	385	15.1%
R5	290	366	390	19.3%
R6	288	362	490	22.3%

3.6. BTMS

3.6.1. Battery

Figure 8 shows the temperature curves of charging and discharging for a single battery under two working conditions of 2 C and 3 C with different materials. W is the control group without PCM, and refers to the temperature of battery charging and discharging in a 25 °C incubator. PA is the temperature of battery charging and discharging under the condition of thermal management using pure paraffin as PCM. This paper mainly studies the thermal management result of RPCM with different content flame-retardants and the influence of kaolinite on the thermal management effect of RPCM. Therefore, it mainly describes the thermal management result of R1, R2, R3, and R6. At 2 C (Figure 8a), it can be found that the maximum temperature of a single cell can reach 47.9 °C without adding any material, and the temperature can be reduced to 40.7 °C by using pure PCM, a decrease of 7.2 °C. The paraffin can also reduce the surface temperature of the LIB, but once the temperature exceeds the melting point of the PCM, the paraffin will melt, posing a threat to the LIB safety. The surface temperature of the battery under the flame-retardant PCM is 38.4–36.9 °C, which is 2.3–3.8 °C lower than that of paraffin wax. The addition of high thermal conductivity material inside the flame-retardant PCM increases the heat transfer rate inside the material, which is beneficial to enhancing the heat dissipation capacity of the LIB. At 3 C (Figure 8b), it can be found that the maximum temperature of a single cell can reach 55.3 °C without adding any material, and the temperature can be reduced to 49.4 °C by using pure paraffin wax, which is 5.9 °C lower. The surface temperature of the LIB under the RPCM is 40.9–37.4 °C, which is 8.5–12 °C lower than that of pure paraffin. It can be observed that after the battery surface temperature increases, the cooling effect of pure

paraffin wax is affected by low thermal conductance, easy leakage, and other shortcomings, and its cooling effect is damaged. However, the flame-retardant PCM can still show a good cooling effect.

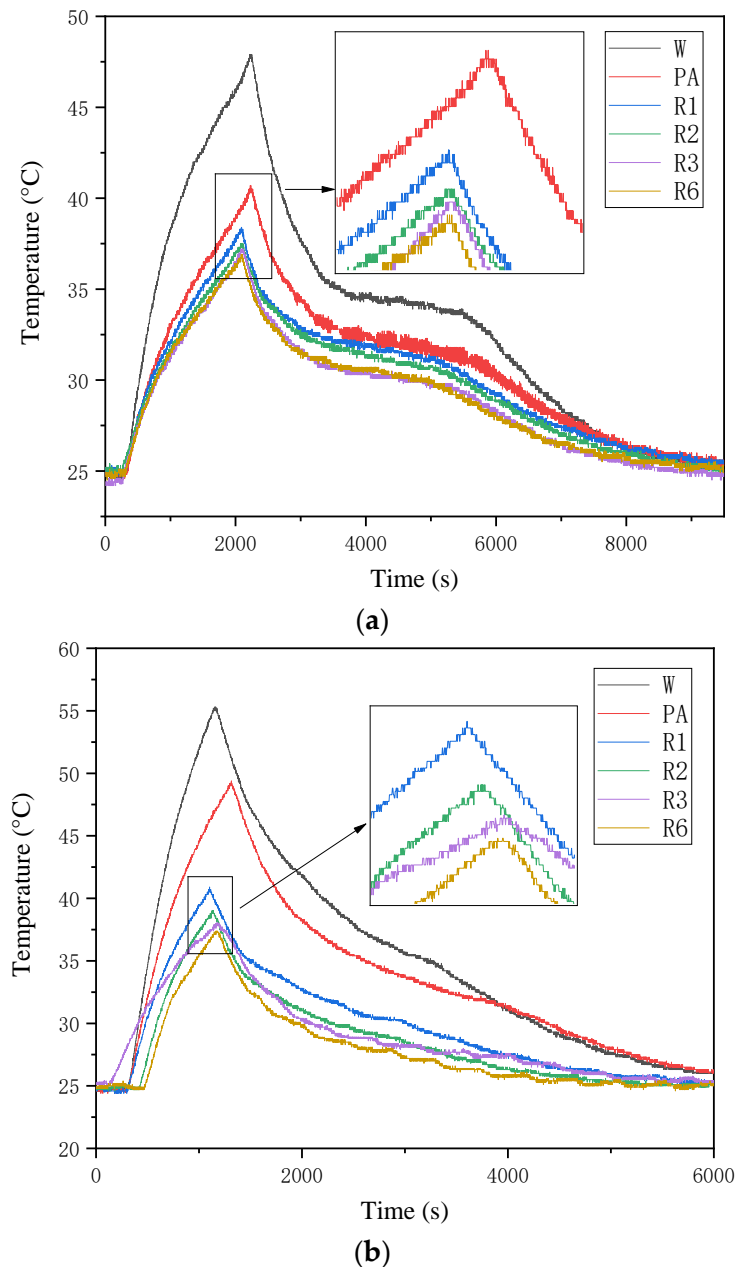


Figure 8. Cell temperature curve (a) 2 C (b) 3 C.

3.6.2. Batteries

Figure 9 shows the charging and discharging temperature changes in the battery string under 1 C, 2 C, and 3 C conditions caused by different materials. The results show that, similar to the cooling effect of a single battery, the RPCM has a good cooling effect on the battery. At 1 C (Figure 9a), it can be found that the peak temperature of a single cell can reach 39.36 °C without adding any material. Using pure PCM can reduce the temperature to 38.2 °C, which is 1.16 °C lower. The surface temperature of the LIB under the RPCM is 37.23–33.89 °C, which is 0.97–4.31 °C lower than that of pure paraffin. It can be found that the cooling effect of PCM at 1c is not obvious, mainly because the melting point of PCM has not been reached, and it cannot play its maximum role. At 2 C (Figure 9b), it can be

found that the maximum temperature of a single cell can reach $58.63\text{ }^{\circ}\text{C}$ without adding any material, and the use of pure PA can decrease the temperature to $54.3\text{ }^{\circ}\text{C}$, which is $4.33\text{ }^{\circ}\text{C}$ lower. The surface temperature of the LIB under the RPCM is $48.15\text{--}47.14\text{ }^{\circ}\text{C}$, which is $6.15\text{--}7.16\text{ }^{\circ}\text{C}$ lower than that of pure paraffin. At 3 C (Figure 9c), it can be found that the peak temperature of a single battery can reach $79.87\text{ }^{\circ}\text{C}$ without adding any material, and the temperature can be reduced to $71.2\text{ }^{\circ}\text{C}$ by using pure PCM, which is $8.67\text{ }^{\circ}\text{C}$ lower. The surface temperature of the LIB under the RPCM is $57.1\text{--}50.28\text{ }^{\circ}\text{C}$, which is $14.1\text{--}20.92\text{ }^{\circ}\text{C}$ lower than that of pure paraffin. Among them, R6 has the most obvious cooling effect. When the discharge current is larger, the battery surface temperature is larger, and the cooling result of PCM is more obvious, indicating that PCM can also absorb heat at high temperature and reduce the battery surface temperature.

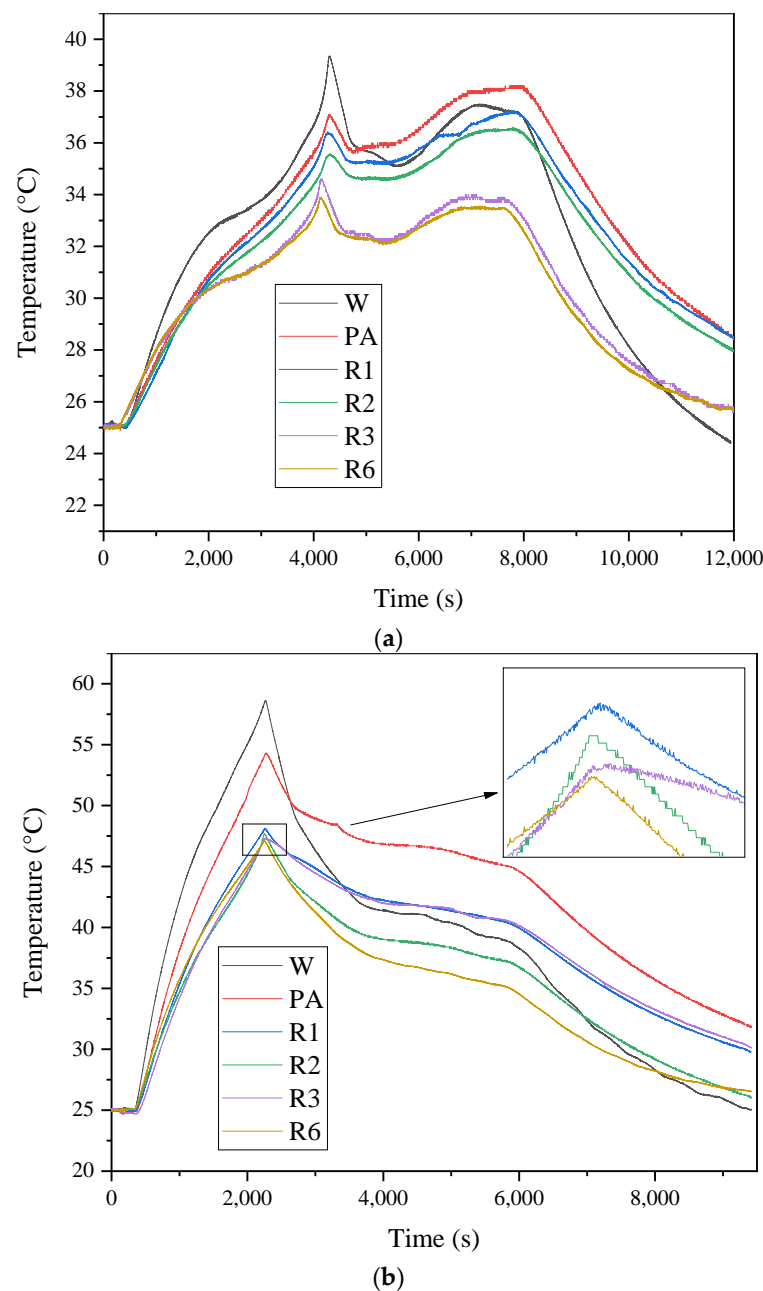


Figure 9. Cont.

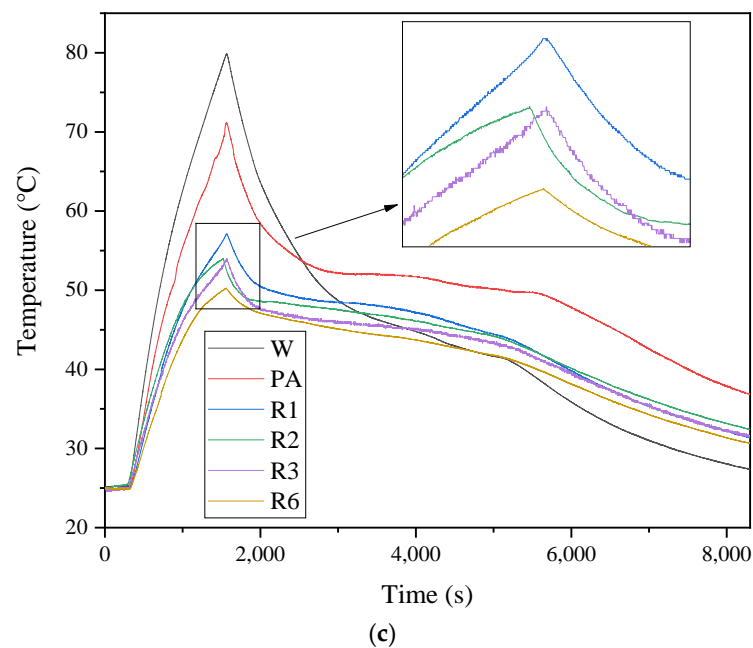


Figure 9. Battery pack temperature curve (a) 1 C, (b) 2 C, (c) 3 C.

Figure 10 shows the temperature difference curve of the battery string. For the battery pack, there will be temperature differences between the cells in the battery string. A long running time may result in large performance differences among battery packs. Therefore, the safety and service life of the entire battery string are seriously affected. During battery string operation, the temperature difference between batteries should not exceed 5 °C [36]. Under natural ventilation, the heat dissipation between batteries is slow and the temperature difference is large. At 1 C condition, the temperature difference without using PCM is also within 5 °C, the highest is 3.4 °C. The addition of flame-retardant PCM makes the temperature difference smaller, up to 1.4 °C. 2 C and 3 C do not use PCMs, and the maximum temperature difference is 4.6 °C and 9.6 °C. The addition of PCM reduces the maximum temperature difference of 2 C to 3.12 °C and 3 C to 4.25 °C. The use of flame-retardant PCM can make the internal temperature difference of lithium-ion battery string less than 5 °C, and thus improve its safety.

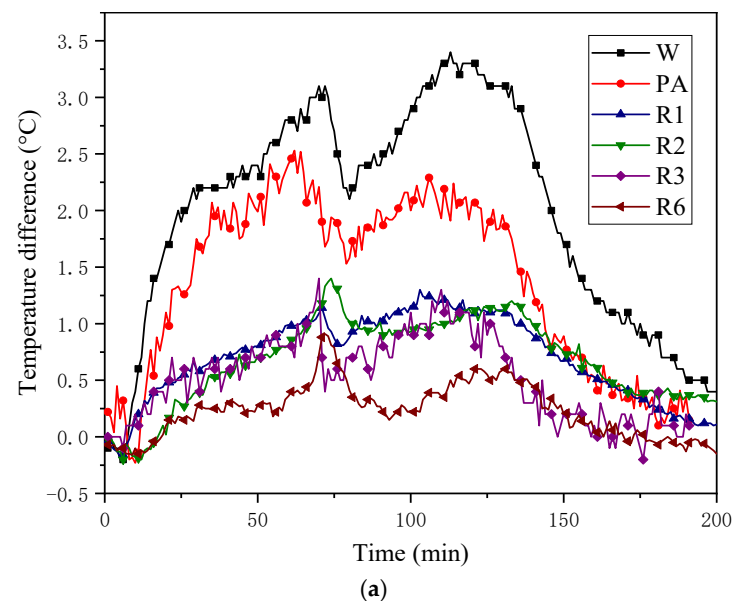


Figure 10. Cont.

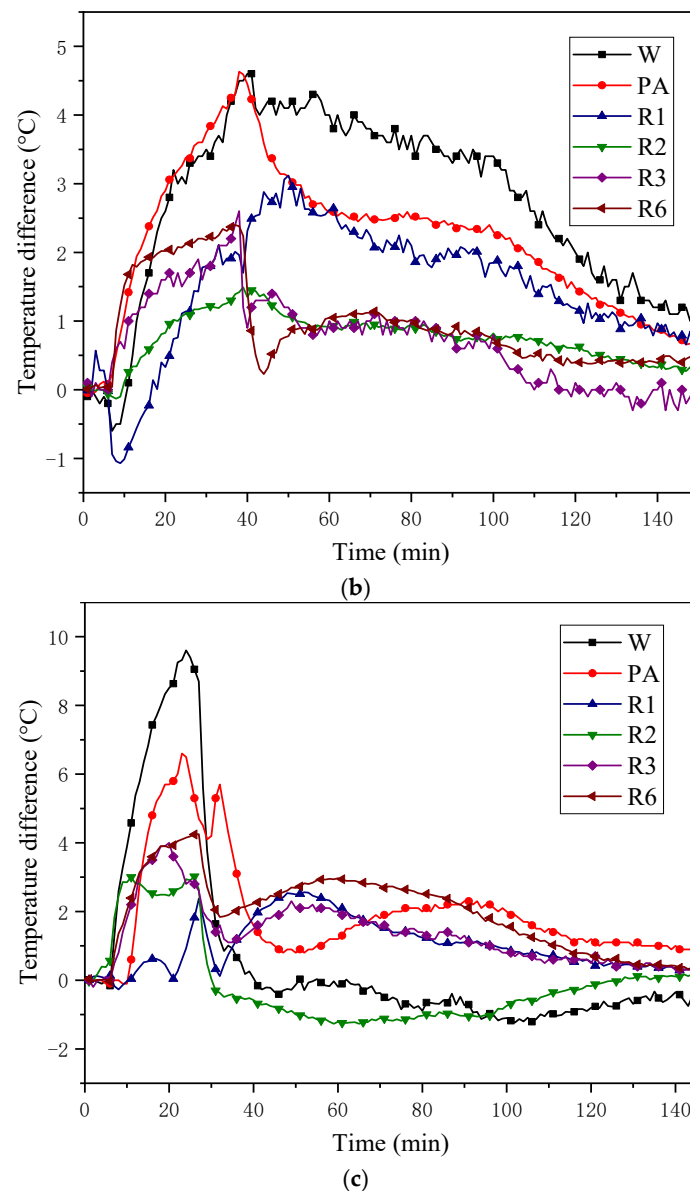


Figure 10. Temperature difference of LIB module curve (a) 1 C (b) 2 C (c) 3 C.

3.7. Fire Retardant Mechanism

In the expansion flame retardant system, it mainly uses the reaction between the expansion flame retardant and the matrix to form a porous expanded carbon layer to achieve flame retardant, in which the polyphosphate is the acid source and the air source, and the CFA is the carbon source. On the one hand, intumescent flame retardants dilute combustible gases by releasing gases such as CO_2 , NH_3 , and H_2O . On the other hand, dehydration forms a carbon layer that blocks the diffusion of oxygen and heat from the combustible gas. In the flame-retardant composite phase change material, paraffin reacts with oxygen to form carboxylic acid, and then dehydrates with the polyphosphate produced by the expansion flame retardant to form an expanded carbon layer. In addition, when kaolin is added to the expansion flame retardant system, it will accumulate on the surface of the material, forming a physical barrier layer [37]. Physical barrier layer and enhanced expanded carbon layer can more effectively prevent the release of combustible gas to the gas phase and the diffusion of oxygen to the material surface, and slow down the degradation rate of materials [38].

4. Conclusions

In this paper, the expansion flame-retardant and kaolinite are used as additives to enhance the flame-retardant property of PCM to prevent the safety problems during the use of PCM. These following conclusions are found.

- (1) The addition of kaolinite can boost the thermal stability of PCM in multiple thermal cycles. It is found that the cooperative use of kaolinite can argument the LOI value of materials by observing the flame retardancy of PCMs.
- (2) The TG results indicate that the addition of flame-retardant can significantly increase the residual carbon content of PCM at 800 °C. The addition of 10% flame-retardant can rise the residual carbon content of the material from 2.3% to 11.8%. The addition of kaolinite also has a synergistic effect, and the residual carbon content of R6 is greater than that of R3.
- (3) Flame-retardant PCMs show good cooling effect in the thermal management of LIB. Compared with pure PA cooling, RPCM reduces the peak temperature of a single cell by 12 °C (3 C) and the peak temperature of the battery module by 20.92 °C (3 C). The temperature difference of the battery module should be kept within 5 °C at 3 C.

There is still a gap between the flame-retardant effect of the phase change material synthesized in this paper and that of the traditional flame-retardant material. Moreover, the inhibitory effect of flame-retardant materials on the thermal runaway propagation of lithium-ion batteries needs to be further verified in experiments.

Author Contributions: Conceptualization, Y.C. (Yilin Cui); Funding acquisition, M.C.; Major experimental work and writing—original draft preparation, Y.C. (Yilin Cui); Writing—review and editing Y.C. (Yin Chen), L.Z., F.Z., L.L., Q.K. and M.C. All authors have read and agreed to the published version of the manuscript.

Funding: This research was funded by the National Natural Science Foundation of China (52204213), the China Postdoctoral Science Foundation (2020M681512), the Science and Technology Program of Fire and Rescue Department Ministry of Emergency Management (2020XFCX33), the Special Scientific Research Project of School of Emergency Management of Jiangsu University (KY-B-09, KY-D-03), and the Project of Research on Educational Reform and Talent Development of School of Emergency Management of Jiangsu University (JG-03-03, JG-04-08).

Data Availability Statement: Data available on request due to restrictions eg privacy or ethical.

Conflicts of Interest: The authors declare no conflict of interest.

References

1. Kong, Q.; Zhu, H.; Huang, S.; Wu, T.; Zhu, F.; Zhang, Y.; Wang, Y.; Zhang, J. Influence of multiply modified FeCu-montmorillonite on fire safety and mechanical performances of epoxy resin nanocomposites. *Thermochim. Acta* **2022**, *707*, 179112. [\[CrossRef\]](#)
2. Ouyang, D.; Weng, J.; Chen, M.; Zhu, Y.; Wang, J.; Wang, Z. A comparative study on safety and electrochemical characteristics of cylindrical lithium-ion cells with various formats. *Process Saf. Environ. Prot.* **2022**, *161*, 126–135. [\[CrossRef\]](#)
3. Weng, J.; Huang, Q.; Li, X.; Zhang, G.; Ouyang, D.; Chen, M.; Yuen, A.C.Y.; Li, A.; Lee, E.W.M.; Yang, W.; et al. Safety issue on PCM-based battery thermal management: Material thermal stability and system hazard mitigation. *Energy Storage Mater.* **2022**, *53*, 580–612. [\[CrossRef\]](#)
4. Weng, J.; Xiao, C.; Ouyang, D.; Yang, X.; Chen, M.; Zhang, G.; Yuen, R.K.K.; Wang, J. Mitigation effects on thermal runaway propagation of structure-enhanced phase change material modules with flame retardant additives. *Energy* **2022**, *239*, 122087. [\[CrossRef\]](#)
5. Ouyang, D.; Weng, J.; Chen, M.; Wang, J.; Wang, Z. Study on topographic, electrochemical, and safety characteristics of lithium-ion cells after long-term storage at abusive-temperature environments. *Int. J. Energy Res.* **2022**, *46*, 11903–11913. [\[CrossRef\]](#)
6. Ouyang, D.; Weng, J.; Chen, M.; Wang, J. What a role does the safety vent play in the safety of 18650-size lithium-ion batteries? *Process Saf. Environ. Prot.* **2022**, *159*, 433–441. [\[CrossRef\]](#)
7. Zhang, X.; Li, Z.; Luo, L.; Fan, Y.; Du, Z. A review on thermal management of lithium-ion batteries for electric vehicles. *Energy* **2022**, *238*, 121652. [\[CrossRef\]](#)
8. Chen, M.; Zhang, S.; Zhao, L.; Weng, J.; Ouyang, D.; Chen, Q.; Kong, Q.; Wang, J. Preparation of thermally conductive composite phase change materials and its application in lithium-ion batteries thermal management. *J. Energy Storage* **2022**, *52*, 104857. [\[CrossRef\]](#)

9. Tete, P.R.; Gupta, M.M.; Joshi, S.S. Developments in battery thermal management systems for electric vehicles: A technical review. *J. Energy Storage* **2021**, *35*, 102255. [\[CrossRef\]](#)
10. Wu, S.; Yan, T.; Kuai, Z.; Pan, W. Thermal conductivity enhancement on phase change materials for thermal energy storage: A review. *Energy Storage Mater.* **2020**, *25*, 251–295. [\[CrossRef\]](#)
11. Al-Zareer, M.; Dincer, I.; Rosen, M.A. A review of novel thermal management systems for batteries. *Int. J. Energy Res.* **2018**, *42*, 3182–3205. [\[CrossRef\]](#)
12. Bibin, C.; Devan, P.K.; Senthil Kumar, S.; Gopinath, S.; Sheeja, R.; Kanthavelkumaran, N.; Gobinath, S.; Ashok, K.G. Thermal performance of Lithium-Ion battery pack using forced air circulation system. *Mater. Today Proc.* **2021**, *46*, 3670–3676. [\[CrossRef\]](#)
13. Ding, Y.; Ji, H.; Wei, M.; Liu, R. Effect of liquid cooling system structure on lithium-ion battery pack temperature fields. *Int. J. Heat Mass Transf.* **2022**, *183*, 122178. [\[CrossRef\]](#)
14. Zhang, J.; Liu, H.; Zheng, M.; Chen, M.; Zhao, L.; Du, D. Numerical study on a preheating method for lithium-ion batteries under cold weather conditions using phase change materials coupled with heat films. *J. Energy Storage* **2022**, *47*, 103651. [\[CrossRef\]](#)
15. Chen, M.; Zhang, S.; Wang, G.; Weng, J.; Ouyang, D.; Wu, X.; Zhao, L.; Wang, J. Experimental Analysis on the Thermal Management of Lithium-Ion Batteries Based on Phase Change Materials. *Appl. Sci.* **2020**, *10*, 7354. [\[CrossRef\]](#)
16. Ianniciello, L.; Biwolé, P.H.; Achard, P. Electric vehicles batteries thermal management systems employing phase change materials. *J. Power Sources* **2018**, *378*, 383–403. [\[CrossRef\]](#)
17. Chen, M.; Cui, Y.; Ouyang, D.; Weng, J.; Liu, J.; Zhao, L.; Wang, J. Experimental study on the hybrid carbon based phase change materials for thermal management performance of lithium-ion battery module. *Int. J. Energy Res.* **2022**, *46*, 17247–17261. [\[CrossRef\]](#)
18. Zou, D.; Liu, X.; He, R.; Zhu, S.; Bao, J.; Guo, J.; Hu, Z.; Wang, B. Preparation of a novel composite phase change material (PCM) and its locally enhanced heat transfer for power battery module. *Energy Convers. Manag.* **2019**, *180*, 1196–1202. [\[CrossRef\]](#)
19. Li, J.; Zuo, X.; Zhao, X.; Li, D.; Yang, H. Stearic acid hybridizing kaolinite as shape-stabilized phase change material for thermal energy storage. *Appl. Clay Sci.* **2019**, *183*, 105358. [\[CrossRef\]](#)
20. Weng, J.; Xiao, C.; Yang, X.; Ouyang, D.; Chen, M.; Zhang, G.; Lee Waiming, E.; Kit Yuen, R.K.; Wang, J. An energy-saving battery thermal management strategy coupling tubular phase-change-material with dynamic liquid cooling under different ambient temperatures. *Renew. Energy* **2022**, *195*, 918–930. [\[CrossRef\]](#)
21. Mei, J.; Shi, G.; Liu, H.; Wang, Z.; Chen, M. Investigation on the optimization strategy of phase change material thermal management system for lithium-ion battery. *J. Energy Storage* **2022**, *55*, 105365. [\[CrossRef\]](#)
22. Qu, J.; Ke, Z.; Zuo, A.; Rao, Z. Experimental investigation on thermal performance of phase change material coupled with three-dimensional oscillating heat pipe (PCM/3D-OHP) for thermal management application. *Int. J. Heat Mass Transf.* **2019**, *129*, 773–782. [\[CrossRef\]](#)
23. Xu, L.; Liu, X.; An, Z.; Yang, R. EG-based coatings for flame retardance of shape stabilized phase change materials. *Polym. Degrad. Stab.* **2019**, *161*, 114–120. [\[CrossRef\]](#)
24. Ribeiro, S.P.S.; Martins, R.C.; Estevão, L.R.M.; Nascimento, M.A.C.; Nascimento, R.S.V. Microscopy as a tool to investigate the influence of ammonium polyphosphate particle size on the flame retardant properties of polymer composites. *Microsc. Res. Tech.* **2020**, *83*, 276–286. [\[CrossRef\]](#)
25. Liu, D.; Hu, A. The Influence of Environmentally Friendly Flame Retardants on the Thermal Stability of Phase Change Polyurethane Foams. *Materials* **2020**, *13*, 520. [\[CrossRef\]](#)
26. Jia, L.; Huang, W.; Zhao, Y.; Wen, S.; Yu, Z.; Zhang, Z. Ultra-light polylactic acid/combination composite foam: A fully biodegradable flame retardant material. *Int. J. Biol. Macromol.* **2022**, *220*, 754–765. [\[CrossRef\]](#)
27. Fan, H.; Gu, X.; Zhang, S.; Liu, F.; Liao, Y.; Tang, W. Synergistic effect between novel triazine-based charring agent and modified kaolinite: An efficient system for fire hazard and aging suppression of epoxy resin. *Polym. Degrad. Stab.* **2022**, *204*, 110109. [\[CrossRef\]](#)
28. Ullah, S.; Ahmad, F.; Shariff, A.M.; Bustam, M.A. Synergistic effects of kaolin clay on intumescent fire retardant coating composition for fire protection of structural steel substrate. *Polym. Degrad. Stab.* **2014**, *110*, 91–103. [\[CrossRef\]](#)
29. Li, Y.-M.; Hu, S.-L.; Wang, D.-Y. Polymer-based ceramifiable composites for flame retardant applications: A review. *Compos. Commun.* **2020**, *21*, 100405. [\[CrossRef\]](#)
30. Isitman, N.A.; Kaynak, C. Nanoclay and carbon nanotubes as potential synergists of an organophosphorus flame-retardant in poly(methyl methacrylate). *Polym. Degrad. Stab.* **2010**, *95*, 1523–1532. [\[CrossRef\]](#)
31. Zia-ul-Mustafa, M.; Ahmad, F.; Ullah, S.; Amir, N.; Gillani, Q.F. Thermal and pyrolysis analysis of minerals reinforced intumescent fire retardant coating. *Prog. Org. Coat.* **2017**, *102*, 201–216. [\[CrossRef\]](#)
32. Weng, J.W.; Ouyang, D.X.; Liu, Y.H.; Chen, M.Y.; Li, Y.P.; Huang, X.Y.; Wang, J. Alleviation on battery thermal runaway propagation: Effects of oxygen level and dilution gas. *J. Power Sources* **2021**, *509*, 230340. [\[CrossRef\]](#)
33. Weng, J.W.; He, Y.P.; Ouyang, D.X.; Yang, X.Q.; Chen, M.Y.; Cui, S.T.; Zhang, G.Q.; Yuen, R.K.K.; Wang, J. Honeycomb-inspired design of a thermal management module and its mitigation effect on thermal runaway propagation. *Appl. Therm. Eng.* **2021**, *195*, 117147. [\[CrossRef\]](#)
34. Feng, C.; Li, Z.; Liang, M.; Huang, J.; Liu, H. Preparation and characterization of a novel oligomeric charring agent and its application in halogen-free flame retardant polypropylene. *J. Anal. Appl. Pyrolysis* **2015**, *111*, 238–246. [\[CrossRef\]](#)

35. Li, L.; Wang, G.; Guo, C. Influence of intumescent flame retardant on thermal and flame retardancy of eutectic mixed paraffin/polypropylene form-stable phase change materials. *Appl. Energy* **2016**, *162*, 428–434. [[CrossRef](#)]
36. Pesaran, A.A. Battery thermal models for hybrid vehicle simulations. *J. Power Sources* **2002**, *110*, 377–382. [[CrossRef](#)]
37. Wang, W.; Pan, H.; Shi, Y.; Pan, Y.; Yang, W.; Liew, K.M.; Song, L.; Hu, Y. Fabrication of LDH nanosheets on β -FeOOH rods and applications for improving the fire safety of epoxy resin. *Compos. Part A Appl. Sci. Manuf.* **2016**, *80*, 259–269. [[CrossRef](#)]
38. Kandare, E.; Di Modica, P.; Chevali, V.S.; Gibson, G.A. Evaluating the heat resistance of thermal insulated sandwich composites subjected to a turbulent fire. *Fire Mater.* **2016**, *40*, 586–598. [[CrossRef](#)]

Disclaimer/Publisher's Note: The statements, opinions and data contained in all publications are solely those of the individual author(s) and contributor(s) and not of MDPI and/or the editor(s). MDPI and/or the editor(s) disclaim responsibility for any injury to people or property resulting from any ideas, methods, instructions or products referred to in the content.